



Original Paper

Reaction characteristics of maximizing light olefins and decreasing methane in C₅ hydrocarbons catalytic pyrolysisMei-Jia Liu^a, Gang Wang^{a,*}, Shun-Nian Xu^a, Tao-Ran Zheng^a, Zhong-Dong Zhang^{b,**}, Sheng-Bao He^b^a State Key Laboratory of Heavy Oil Processing, China University of Petroleum, Beijing, 102249, China^b Petrochemical Research Institute, PetroChina, Beijing, 102206, China

ARTICLE INFO

Article history:

Received 9 June 2022

Received in revised form

31 July 2022

Accepted 30 November 2022

Available online 5 December 2022

Edited by Jia-Jia Fei

Keywords:

n-Pentane

1-Pentene

Catalytic pyrolysis

Light olefins

Methane

ABSTRACT

When converting C₅ hydrocarbons to light olefins by catalytic pyrolysis, the generation of low value-added methane will affect the atomic utilization efficiency of C₅ hydrocarbons. To improve the atomic utilization efficiency, different generation pathways of light olefins and methane in the catalytic pyrolysis of C₅ hydrocarbons were analyzed, and the effects of reaction conditions and zeolite types were investigated. Results showed that light olefins were mainly formed by breaking the C₂–C₃ bond in the middle position, while methane was formed by breaking the C₁–C₂ bond at the end. Meanwhile, it was discovered that the hydrogen transfer reaction could be reduced by about 90% by selecting MTT zeolite with 1D topology and FER zeolite with 2D topology under high weight hourly space velocity (WHSV) and high temperature operations, thus leading to the improvement of the light olefins selectivity for the catalytic pyrolysis of *n*-pentane and 1-pentene to 55.12% and 74.60%, respectively. Moreover, the fraction ratio of terminal C₁–C₂ bond cleavage was reduced, which would reduce the selectivity of methane to 6.63% and 1.83%. Therefore, zeolite with low hydrogen transfer activity and catalytic pyrolysis process with high WHSV will be conducive to maximize light olefins and to decrease methane.

© 2023 The Authors. Publishing services by Elsevier B.V. on behalf of KeAi Communications Co. Ltd. This is an open access article under the CC BY-NC-ND license (<http://creativecommons.org/licenses/by-nc-nd/4.0/>).

1. Introduction

With the rapid transition of refineries to refining-petrochemical integration, it is an irresistible trend to convert the excess light gasoline fraction into light olefins by catalytic pyrolysis (Corma et al., 2004, 2013, 2017; Li et al., 2007; Wang et al., 2008; Sundberg et al., 2018). The ratio of carbon to hydrogen determines that light gasoline (molar ratio of C/H = 0.4–0.5) is suitable for the production of light olefins (molar ratio of C/H = 0.5), such as ethylene and propylene. The C₅ hydrocarbons in light gasoline have short carbon chains and require more energy input to produce light olefins through molecular reconstruction, thus high temperature is a preferred operation condition. However, more methane will be

generated at high temperature which will reduce the selectivity of light olefins and will further affect the atomic utilization efficiency of C₅ hydrocarbons (Kubo et al., 2012; Zhang et al., 2016, 2021).

In recent years, researchers have analyzed the mechanism of catalytic pyrolysis to produce light hydrocarbons (Chu et al., 2016; Lin et al., 2014, 2015). Hou et al. (2017) analyzed the cracking reaction pathways of *n*-pentane over zeolites and found that monomolecular cracking routes were mainly initiated by the attack of acid sites on C–H or C₂–C₃ bonds. Thivasasith et al. (2019) found that the energy barrier of *n*-pentane cracking reaction path 1 (C₅H₁₂ → C₂H₆ + C₃H₆) over zeolite was 0.5–6.7 kcal mol⁻¹ lower than that of the cracking reaction path 2 (C₅H₁₂ → C₂H₄ + C₃H₈). Huang et al. (2015) analyzed the product distribution of catalytic cracking of pentene, and they proposed that pentene was cracked by monomolecular and bimolecular cracking reactions. Bimolecular cracking reactions (2C₅H₁₀ → C₄H₈ + C₆H₁₂; 2C₅H₁₀ → C₃H₆ + C₇H₁₄) were inclined to occur at low temperature, while monomolecular cracking reactions (C₅H₁₀ → C₂H₄ + C₃H₆) were dominated at high temperature. Wei et al. (2014) used *n*-octane as a model compound to study the formation of methane in naphtha catalytic pyrolysis.

* Corresponding author. State Key Laboratory of Heavy Oil Processing, China University of Petroleum, Beijing, 102249, China.

** Corresponding author. Petrochemical Research Institute, PetroChina, Beijing, 102206, China.

E-mail addresses: wanggang@cup.edu.cn (G. Wang), zhangzhongdong@petrochina.com.cn (Z.-D. Zhang).

Their results showed that when the reaction temperature was in the range of 600–700 °C, the CH₄ generation was attributed to the combined action of hydrocarbon radical and carbonium ion reactions. Meanwhile, the effects of the process parameters on methane in naphtha catalytic pyrolysis were investigated. It was found that the selectivity of methane would be reduced by increasing the mass ratio of catalyst to oil and shortening the reaction time. However, there still lacks the reports related to the comprehensive analysis of the generation pathways of light olefins and methane in the catalytic pyrolysis of light hydrocarbons.

Some researchers also analyzed different zeolite types for the catalytic pyrolysis of light hydrocarbons (Feng et al., 2022; Miyaji et al., 2015; Zhu et al., 2005). Corma et al. (1985) found that *n*-heptane cracking over HZSM-5 and HUSY zeolites had different product composition distributions, and the selectivity of light olefins was high on HZSM-5 zeolite. Hou et al. (2017) found that compared with HZSM-35 and H-Beta zeolites, *n*-pentane had high light olefins selectivity on HZSM-5 zeolite. Rownaghi et al. (2012) proposed that zeolites with small crystal size were favorable for the conversion of *n*-hexane, and the low acid concentration on the external surface of the catalyst helped improve the selectivity of light olefins. Bortnovsky et al. (2005) proposed that the ZSM-5 and ZSM-11 zeolites with low acid concentration and strong acids would lead to high iso-pentene conversion and high yield of C₂–C₄ olefins. The type of zeolite both affects the selectivity of light olefins and methane in the catalytic pyrolysis of light hydrocarbons. However, limited reports were focused on the study of the effects of zeolite types on the formation of light olefins and methane in catalytic pyrolysis.

In this work, the catalytic pyrolysis reaction mechanism of C₅ hydrocarbons (*n*-pentane and 1-pentene) is analyzed to realize the efficient conversion of light olefins and reduce the generation of low value-added methane. At the same time, the effects of reaction conditions and zeolite types on the catalytic pyrolysis of C₅ hydrocarbons are explored. This work will provide guidance for the efficient catalytic pyrolysis of C₅ hydrocarbons to light olefins in the industry.

2. Experimental section

2.1. Feedstock and catalyst

The *n*-pentane and 1-pentene are representative C₅ hydrocarbons in light gasoline, so they were used as feedstock in the catalytic pyrolysis. The *n*-pentane (99 wt%) and 1-pentene (98 wt%) were produced by Shanghai Aladdin Biochemical Technology Co., Ltd.

To study the effect of zeolite types on the catalytic pyrolysis, different industrial zeolites with MTT, FER, MFI, BEA, and FAU topologies were selected in this study, which were provided by Petrochemical Research Institute, PetroChina, Beijing.

2.2. Catalysts characterization

The structural properties of zeolites were tested by nitrogen adsorption-desorption on ASAP 2460 instrument. The samples were pretreated under vacuum atmosphere at 300 °C for 4 h, and the adsorbed nitrogen was pretreated at –196 °C. The specific surface area of the zeolites was calculated using the BET equation, and the pore volume was calculated using the t-plot method. The acid properties of zeolites were determined by NH₃-TPD on an Autochem 2920 apparatus. Zeolite (20–40 mesh) with weight of 0.1 g was pretreated at 600 °C for 0.5 h with N₂ stream (30 mL/min). When the temperature was reduced to 100 °C, the sample was treated with 5% NH₃/N₂ (30 mL/min) for 0.5 h. Subsequently, the

temperature was increased from 100 °C to 600 °C at a rate of 10 °C/min to remove chemically adsorbed NH₃. The desorbed NH₃ was recorded by a thermal conductivity detector.

2.3. Reaction equipment and product analysis

The catalytic pyrolysis of C₅ hydrocarbons was performed in a micro-fixed bed reactor at an ambient pressure (Fig. 1). The zeolite (1–5 g) was in the middle part of the reactor, and it was pretreated at 200 °C under N₂ flow with flow rate of 20 mL/min for 30 min. The reactor was heated to the reaction temperature for 10 min. The feed (3 g) was injected at a constant speed by a micro syringe pump into the reactor, under the N₂ atmosphere (20 mL/min) maintained for 30 min. After the product was cooled, the liquid was collected in a narrow-necked bottle, and the gas was collected by a drainage method. Finally, the gas, liquid, and zeolite were analyzed in the following part.

The reaction products were analyzed by various instruments. The composition of gas products was analyzed by gas chromatography (GC, Agilent 6890N) with the flame ionization detector (FID) and a capillary column (SiO₂, 30 m 0.32 mm). The composition of liquid products was analyzed by another GC (Agilent 6890) with a methyl silicone column (50 m×0.2 mm×0.5 μm). The coke content on zeolite was analyzed by an infrared high frequency carbon sulfur analyzer (HIR-944B).

After the detailed analysis of the reaction products, the calculation formulas for the conversion of C₅ hydrocarbons and the selectivity of product (i) are shown in Eqs. (1) and (2), where Y_i is the yield of product i.

$$\text{Conversion} = 1 - \frac{W_{\text{unreacted feed}}}{W_{\text{feed}}} \times 100\% \quad (1)$$

$$\text{Selectivity} = \frac{Y_i}{\text{Conversion}} \times 100\% \quad (2)$$

3. Results and discussion

3.1. Structure and acidity of different zeolites

The structural properties and acid properties of different zeolites are listed in Table 1 and Table 2, respectively. Table 1 shows that the maximum spherical diameter contained in zeolite was in the order of MTT < FER < MFI < BEA < FAU. MTT zeolite had the smallest micropore volume, whereas FAU zeolite had the largest micropore volume. Table 2 shows that there were differences in the acid content of the six zeolites. BEA zeolite had the highest total acid content of 0.650 mmol g⁻¹, whereas MFI zeolite had the lowest total acid content of 0.218 mmol g⁻¹.

3.2. Analysis of reaction mechanism of C₅ catalytic pyrolysis

It is of great significance for optimizing the product distribution of catalytic pyrolysis by analyzing the reaction mechanism of the catalytic pyrolysis of C₅ hydrocarbons, especially the formation mechanism of light olefins and methane. When the reaction temperature was higher than 550 °C, the C₅ hydrocarbons may undergo thermal cracking in the catalytic pyrolysis (Hou et al., 2019; Liu et al., 2021b; Zhang et al., 2016). Therefore, the thermal cracking and catalytic pyrolysis experiments of C₅ hydrocarbons were carried out under weight hourly space velocity (WHSV) of 216 h⁻¹ and the reactor was filled with quartz sand and MFI zeolite, respectively.

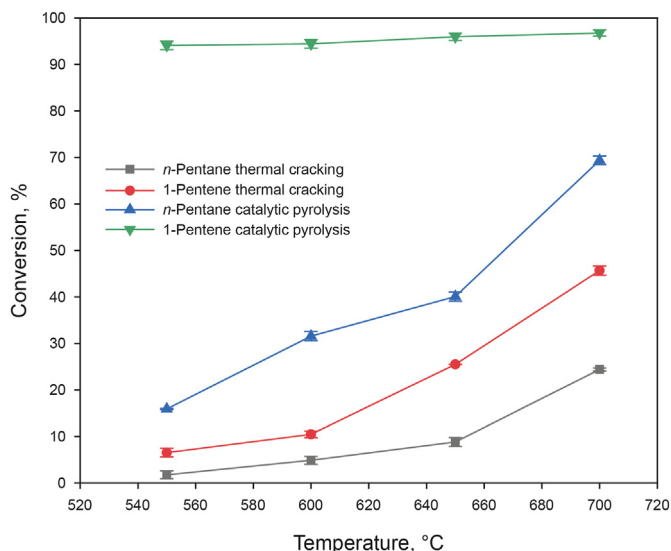
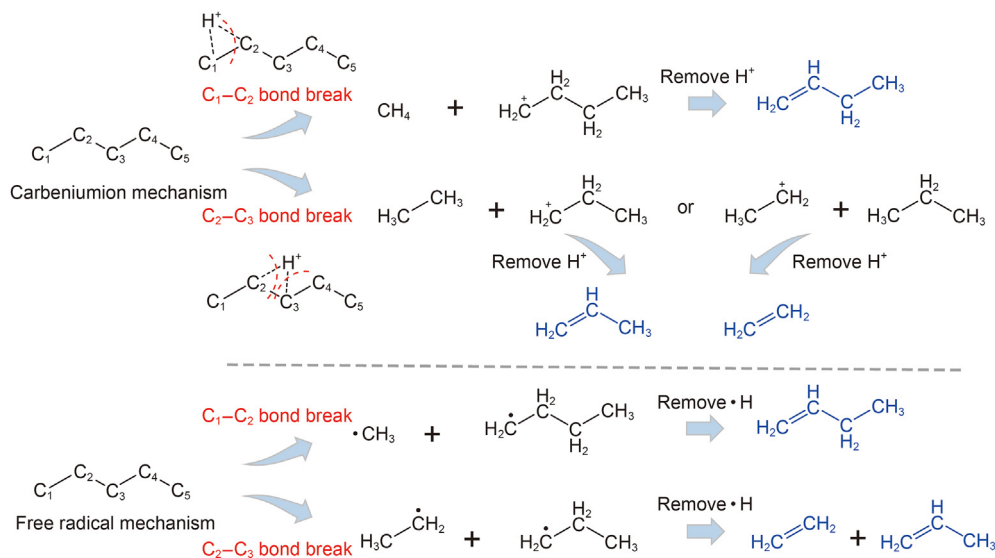


Fig. 2. Conversion of thermal cracking and catalytic pyrolysis of C_5 hydrocarbons.

2019; Krannila et al., 1992; Liu et al., 2021a), the monomolecular cracking reaction pathways for the catalytic pyrolysis of n -pentane in producing light olefins are shown in Scheme 1. When the Bronsted acid center H^+ of zeolite attacks the C_1-C_2 and C_2-C_3 bonds of n -pentane, pentacoordinate carbanions are formed. Pentacoordinate carbanions are cracked in producing ethyl carbenium ion, propyl carbenium ion, and butyl carbenium ion. These carbenium ions could remove H^+ to generate ethylene, propylene and butene. Meanwhile, n -pentane could also produce light olefins through the free radical mechanism during catalytic pyrolysis. When the C_1-C_2 and C_2-C_3 bonds of n -pentane undergo homolysis, ethyl radical, propyl radical, and butyl radical can be generated. Subsequently, the hydrogen radicals could be removed to produce ethylene, propylene, and butene. In addition, n -pentane could also generate pentyl carbenium ion or pentyl radical through $C-H$ bond cleavage, and then further generate light olefins through C_1-C_2 and C_2-C_3 bonds cleavage.

To further confirm the cracking reaction pathways of n -pentane,



Scheme 1. Reaction pathways for the catalytic pyrolysis of n -pentane in producing light olefins.

the molar percentages of the main products for the catalytic pyrolysis of n -pentane at different reaction temperatures are shown in Fig. 3. At 550 °C, the molar percentage of CH_4 was similar to that of $C_4H_{10}+C_4H_8$, and the molar percentage of $C_2H_6+C_2H_4$ was similar to that of $C_3H_8+C_3H_6$. This result was consistent with the monomolecular cracking reaction mechanism of n -pentane (Scheme 1, $C_5H_{12} \rightarrow CH_4 + C_4H_8/C_4H_{10}$; $C_5H_{12} \rightarrow C_2H_6 + C_3H_6/C_2H_4 + C_3H_8$). However, when the reaction temperature increased, the mole percentages of $C_3H_8+C_3H_6$ and $C_4H_{10}+C_4H_8$ decreased, and were smaller than the mole percentages of $C_2H_6+C_2H_4$ and CH_4 , respectively, which indicated that $C_3H_8+C_3H_6$ and $C_4H_{10}+C_4H_8$ might undergo secondary cracking and other side reactions at high temperatures.

According to the previous analysis on the reaction mechanism of catalytic pyrolysis of olefins (Lin et al., 2014, 2015; Liu et al., 2021b; Xu, 2013), the monomolecular cracking reaction pathways for the catalytic pyrolysis of 1-pentene in producing light olefins are shown in Scheme 2. When the Bronsted acid center H^+ of zeolite attacks the C_1-C_2 bond of 1-pentene, pentacoordinate carbanion is

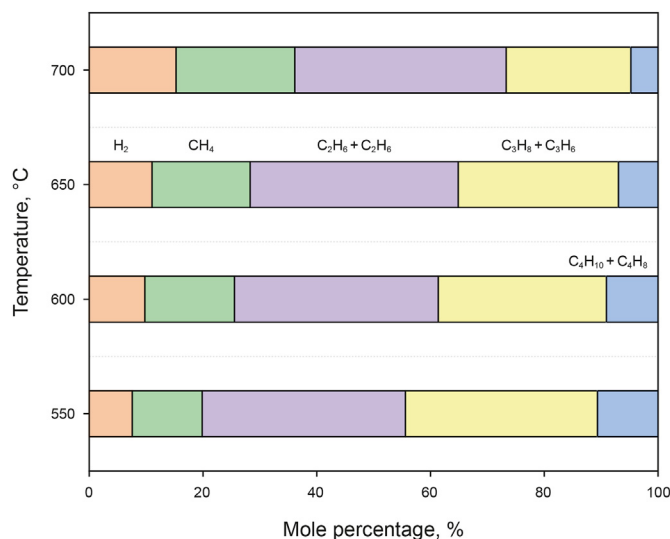
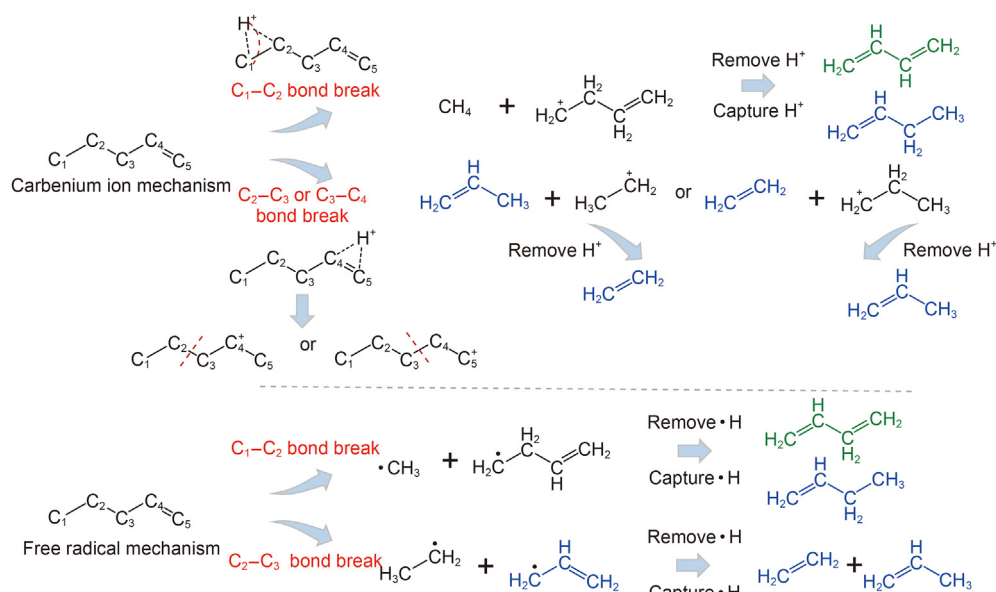


Fig. 3. Molar percentage of the main products for the catalytic pyrolysis of n -pentane.



Scheme 2. Reaction pathways for the catalytic pyrolysis of 1-pentene in producing light olefins.

formed. Pentacoordinate carbanion is cracked to produce butenyl carbenium ion, and carbenium ion could remove the H^+ or capture H^- to generate 1, 3-butadiene or butene. When the Bronsted acid center H^+ of zeolite attacks the C_2-C_3 bond of 1-pentene, pentyl carbenium is formed. Pentyl carbenium generates ethylene and propyl carbenium ion or ethyl carbenium ion and propylene via β -scission, and carbenium ions could remove the H^+ to generate propylene and ethylene. Similarly, 1-pentene could also produce light olefins through the free radical mechanism during catalytic pyrolysis. When the C_1-C_2 and C_2-C_3 bonds undergo homolysis, ethyl radical, propenyl radical, and butenyl radical are generated. These free radicals could remove or capture hydrogen radicals to produce ethylene, propylene, butene, and 1, 3-butadiene. In addition, 1-pentene could also generate pentenyl carbonium ion or pentenyl radical through $C-H$ bond cleavage, and then further generate light olefins through C_1-C_2 and C_2-C_3 bonds cleavage. It is found that ethylene and propylene are generated by the break of C_2-C_3 bond, and butene is generated by the break of C_1-C_2 bond based on the analysis of the formation pathways of light olefins.

To further confirm the cracking reaction pathways of 1-pentene, the molar percentages of the main products for the catalytic pyrolysis of 1-pentene at different reaction temperatures are shown in Fig. 4. When the reaction temperature was lower than 700°C , the mole percentage of $C_4H_8+C_4H_{10}+C_4H_6$ was significantly higher than that of CH_4 , and the mole percentage of $C_3H_8+C_3H_6$ was higher than that of $C_2H_6+C_2H_4$. Huang et al. (2015) proposed that bimolecular cracking reactions ($2C_5H_{10} \rightarrow C_4H_8+C_6H_{12}$; $2C_5H_{10} \rightarrow C_3H_6+C_7H_{14}$) were inclined to occur at low temperature, while monomolecular cracking reactions ($C_5H_{10} \rightarrow C_2H_4+C_3H_6$) were dominated at high temperature. Therefore, the results at low temperature might be caused by bimolecular cracking. However, the molar percentage of CH_4 was similar to that of $C_4H_{10}+C_4H_8$, and the molar percentage of $C_2H_6+C_2H_4$ was similar to that of $C_3H_8+C_3H_6$ at 700°C . This result could further verify the monomolecular cracking reaction mechanism of 1-pentene ($Scheme\ 2$, $C_5H_{10} \rightarrow CH_4+C_4H_8/C_4H_{10}/C_4H_6$; $C_5H_{10} \rightarrow C_2H_4+C_3H_6$).

3.2.2. Analysis of the formation mechanism of methane

According to the analysis of the cracking reaction pathways of n -pentane and 1-pentene (Scheme 1 and Scheme 2) and the

experimental results (Figs. 3 and 4), the molar percentage of CH_4 was similar to that of $C_4H_{10}+C_4H_8$ for the catalytic pyrolysis of C_5 hydrocarbons. Therefore, the generation pathways of methane could be summarized as shown in Scheme 3. When the C_1-C_2 bond at the end of n -pentane and 1-pentene is attacked by the Bronsted acid center H^+ of zeolite, pentacoordinate carbanion is generated. As a result, pentacoordinate carbanion is cracked in generating methane. Meanwhile, methane also could be generated by free radical mechanism. When the C_1-C_2 bonds at the end of the n -pentane and 1-pentene undergo homolysis, methyl radical, butyl radical and butenyl radical could be generated. The methyl radical could capture hydrogen radical from other hydrocarbon molecules in generating methane, the butyl radical could capture or remove hydrogen radicals in generating butane or butene, and the butenyl radical could capture or remove hydrogen radicals to generate butene or 1, 3-butadiene. It is found that methane is generated by the break of the C_1-C_2 bond at the end according to the analysis of

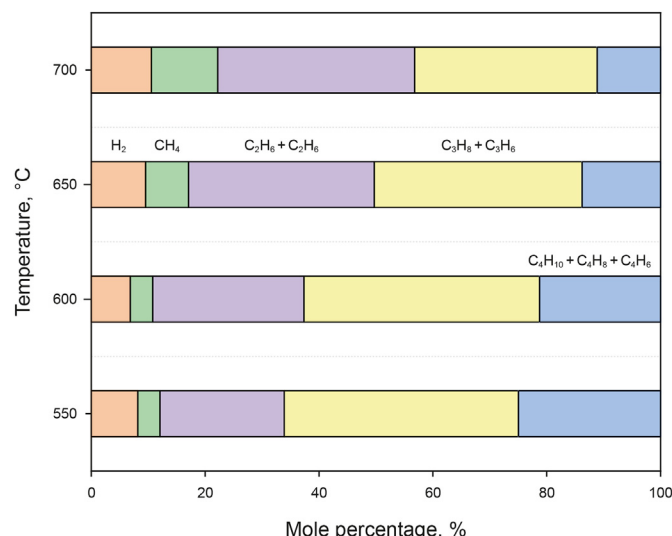
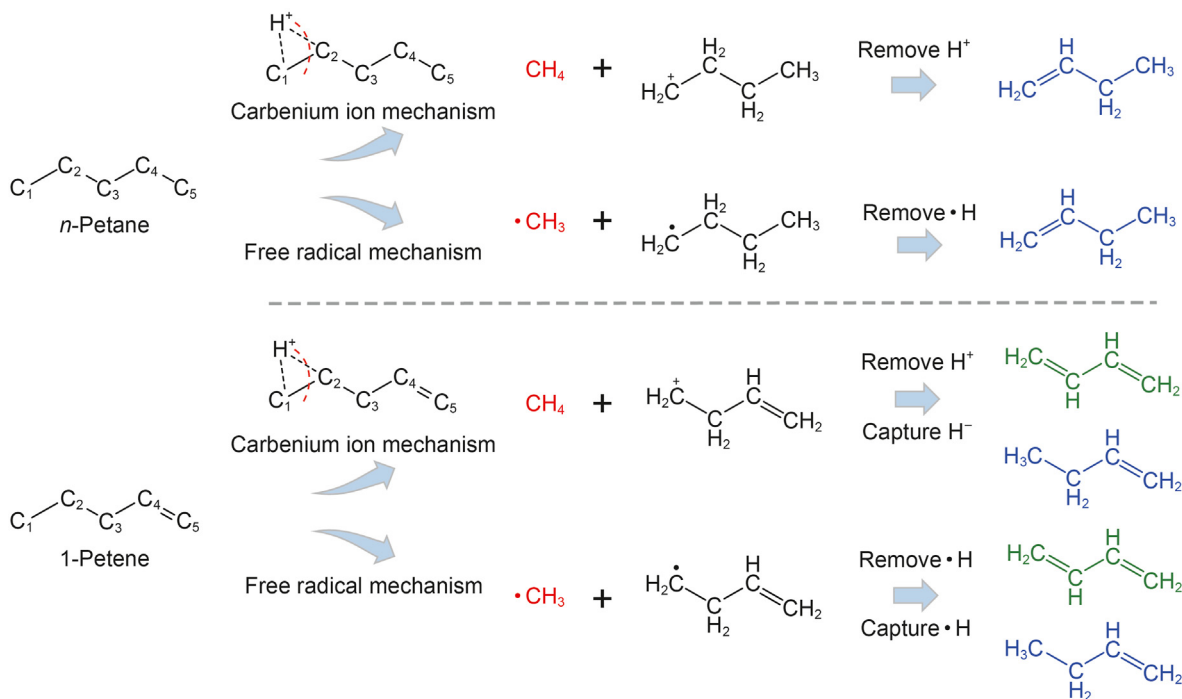


Fig. 4. Molar percentage of the main products for the catalytic pyrolysis of 1-pentene.



the formation pathways of methane.

To quantitatively reveal the breaking ratio of C_1-C_2 bond in the catalytic pyrolysis of C_5 hydrocarbons, the cracking reaction pathways of C_5 hydrocarbons were analyzed. Assuming that the methane is generated by the C_1-C_2 bond break ($C_5H_{12} \rightarrow CH_4 + C_4H_8/C_4H_{10}$; $C_5H_{10} \rightarrow CH_4 + C_4H_8/C_4H_{10}/C_4H_6$), propane and propylene are generated by the break of C_2-C_3 bond ($C_5H_{12} \rightarrow C_2H_6 + C_3H_6/C_2H_4 + C_3H_8$; $C_5H_{10} \rightarrow C_2H_4/C_2H_6 + C_3H_6/C_3H_8$), and hydrogen is generated by the break of $C-H$ bond break ($C_5H_{12} \rightarrow H_2 + C_5H_{10}$; $C_5H_{10} \rightarrow H_2 + C_5H_8$). Therefore, the cleavage ratio of C_1-C_2 bond, C_2-C_3 bond, and $C-H$ bond could be represented by the molar ratio of methane, propane+propylene, and hydrogen. The experimental results of *n*-pentane at 550 °C and 1-pentene at 700 °C were selected to analyze the cracking reaction pathways of C_5 hydrocarbons, because they were consistent with the monomolecular cracking according to the analysis in sections 3.2.1 and 3.2.2. Scheme 4 shows that the break ratio of C_1-C_2 bond, C_2-C_3 bond, and $C-H$ bond was 23:63:14 and 22:59:19 for *n*-pentane and 1-pentene, respectively. This result indicated that the C_2-C_3 bond was mainly broken in the middle, followed by the C_1-C_2 bond at the end, while the $C-H$ bond is the most difficult to break. Considering that the breakage ratio of terminal C_1-C_2 bond is high, thus reducing the break ratio of the C_1-C_2 bond at the end could inhibit the formation of methane for the catalytic pyrolysis of C_5 hydrocarbons.

3.3. Effect of reaction conditions on the catalytic pyrolysis of C_5

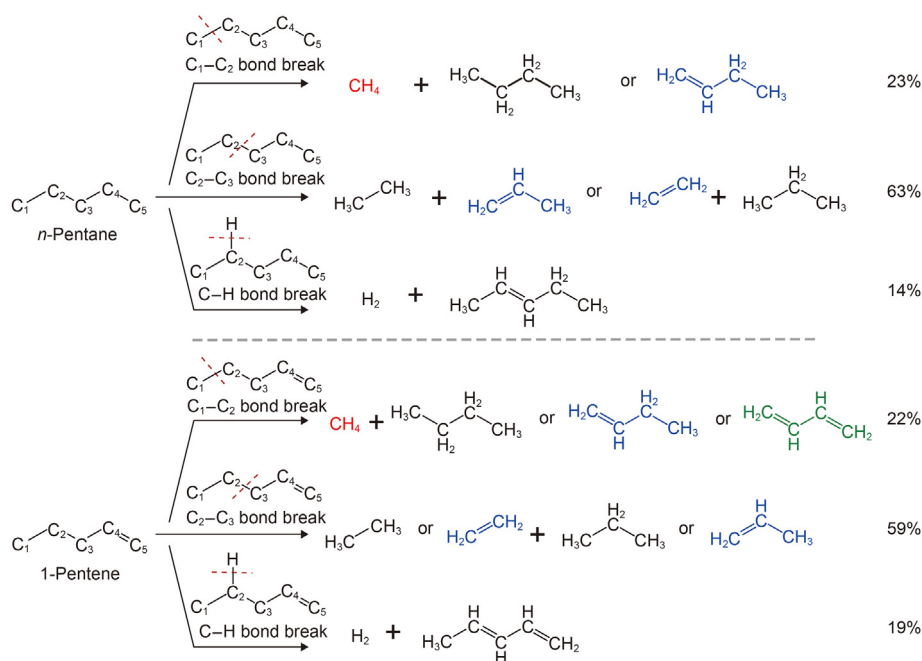
3.3.1. Effect of reaction temperature

The reaction conditions, especially the reaction temperature, play an important role in the product distribution. Therefore, the effects of reaction temperature on the catalytic pyrolysis of C_5 hydrocarbons were studied when the WHSV was 216 h^{-1} . As shown in Fig. 5a, with the increase in reaction temperature, the selectivity of light olefins (ethylene+propylene+butene) in the catalytic pyrolysis of *n*-pentane firstly increased and then decreased. At 650 °C,

the selectivity of light olefins showed the highest value of 46.28%. The selectivity of light olefins in the catalytic pyrolysis of 1-pentene increased by increasing the reaction temperature. When the reaction temperature increased from 550 °C to 700 °C, the selectivity of light olefins increased from 46.30% to 67.68%.

Meanwhile, the selectivity of ethane+propane+butane decreased under higher reaction temperature (Fig. 5b). Given that the hydrogen transfer reaction could convert light olefins into light alkanes (Potapenko et al., 2016), the hydrogen transfer coefficient (HTC, ratio of the total molar selectivity of propane and butane to the molar selectivity of propylene and butene) for catalytic pyrolysis of C_5 hydrocarbons was analyzed in Fig. 5c. When the reaction temperature increased, the HTC value of *n*-pentane and 1-pentene catalytic pyrolysis decreased, indicating that the hydrogen transfer reaction could be reduced at high temperature, thus further improve the selectivity of light olefins, and decrease the selectivity of light alkanes. The mass ratio of propene to ethylene (P/E) of the catalytic pyrolysis of C_5 hydrocarbons was analyzed in Fig. 5d. The P/E of the catalytic pyrolysis of *n*-pentane and 1-pentene decreased by increasing the reaction temperature, which was consistent with the literature (Kubo et al., 2012).

The effects of reaction temperature on methane selectivity and mass ratio of methane to light olefins are shown in Fig. 6. The selectivity of methane increased with the increase in reaction temperature. Additionally, the mass ratio of methane to light olefins also showed increasing trend under higher reaction temperature, indicating that the increase rate of methane was higher than that of light olefins with the increase in reaction temperature. From the perspective energy of the $C-C$ chemical bond, the energy of the $C-C$ bond at the end of C_5 hydrocarbons was about 10 kJ/mol higher than that of the $C-C$ bond at the middle position (Luo, 2005). Moreover, methane is formed through the break of the $C-C$ bond at the end. Therefore, fracture of $C-C$ bond at the end would be promoted by increasing the reaction temperature, which would improve the selectivity of methane.



Scheme 4. Cracking reaction pathways of C₅ hydrocarbons.

3.3.2. Effect of WHSV

To investigate the effect of WHSV on the catalytic pyrolysis of C₅ hydrocarbons, the experiments on catalytic pyrolysis of C₅ hydrocarbons were carried out by changing the feeding rate. Considering the selectivity of light olefins and the selectivity of methane, the reaction temperature was 650 °C. Fig. 7 shows the conversion of C₅ hydrocarbons catalytic pyrolysis at different WHSVs. The conversion of the C₅ hydrocarbons catalytic pyrolysis decreased with the increase in WHSV. When WHSV increased from 6 h⁻¹ to 216 h⁻¹, the conversion of the catalytic pyrolysis of *n*-pentane and 1-pentene decreased from 91.54% and 99.93% to 40.10% and 95.96%, respectively.

However, with the increase in WHSV, the selectivity of light olefins for the catalytic pyrolysis of C₅ hydrocarbons increased and the selectivity of methane decreased as shown in Fig. 8a and b. When WHSV increased from 6 h⁻¹ to 216 h⁻¹, the selectivity of light olefins for the catalytic pyrolysis of *n*-pentane and 1-pentene increased from 38.49% and 38.32% to 46.28% and 62.58% respectively, and the selectivity of methane decreased from 10.83% and 11.66% to 7.80% and 2.83%, respectively. Fig. 8c shows that the selectivity of light alkanes (ethane+propane+butane) for the catalytic pyrolysis of the C₅ hydrocarbons changed slightly with the increase in WHSV. However, with the decrease in WHSV, the selectivity of propane and butane both decreased and the selectivity of ethane increased, indicating that reducing the WHSV could increase the reaction time, thereby promoting the cracking of propane and butane to methane and ethane. Table 3 shows that the shorter the carbon chain of the hydrocarbon molecule, the higher the methane selectivity of its cracking. Therefore, improving the WHSV would lead to a decrease in methane selectivity, because the cracking of propane and butane was promoted.

The hydrogen transfer reaction in the catalytic pyrolysis of C₅ hydrocarbons was analyzed. Fig. 8d shows that HTC decreased with the increase in WHSV. Therefore, with the increase in WHSV, the selectivity of light olefins increased while the selectivity of

methane decreased, because of the reduction of occurrence of side reactions, including hydrogen transfer and secondary cracking reactions. Fig. 8e shows that increasing WHSV could improve the P/E. Therefore, higher WHSV was improved to facilitate C₅ catalytic pyrolysis on the premise of ensuring that C₅ hydrocarbons exhibited a certain conversion, which was conducive to the production of light olefins, and inhibit the formation of methane.

3.4. Effect of zeolite types on the catalytic pyrolysis of C₅

Zeolite also plays a critical role in the catalytic pyrolysis process (Koyama et al., 2010; Primo and Garcia, 2014; Sadrameli, 2016). The selection of appropriate zeolite is important for the efficient conversion of hydrocarbons by catalytic pyrolysis (Bortnovsky et al., 2005; Corma et al., 1999; Jung et al., 2004; Miyaji et al., 2015; Zhu et al., 2005). Therefore, zeolites with different topologies, such as MTT, FER, MFI, BEA, and FAU, were selected to study the catalytic pyrolysis of C₅ hydrocarbons in this section. When the reaction temperature was 650 °C and the WHSV was 216 h⁻¹, the conversion of *n*-pentane and 1-pentene over different zeolites was controlled by changing the amount of zeolite at about 45% and 95%, respectively, as shown in Fig. 9.

Fig. 10a shows that the selectivity of light olefins for *n*-pentane catalytic pyrolysis on MTT and FER zeolites was 55.12% and 48.11%, respectively. Meanwhile, the selectivity of light olefins for 1-pentene catalytic pyrolysis on MTT and FER zeolites was 74.60% and 63.00%, respectively. Fig. 10b shows that the HTC of the catalytic pyrolysis of C₅ hydrocarbons on MTT zeolite and FER zeolite was reduced to about 90% compared with that on FAU zeolite. According to the structural properties of different zeolites (Table 2), the maximum spherical diameter contained in MTT zeolite with 1D topology and in FER zeolite with 2D topology was small. Moreover, the diffusion of hydrocarbon molecules in small pore zeolite requires a high diffusion energy barrier (as shown in Table 4) (Yuan et al., 2011). Therefore, zeolite with small pore size could inhibit

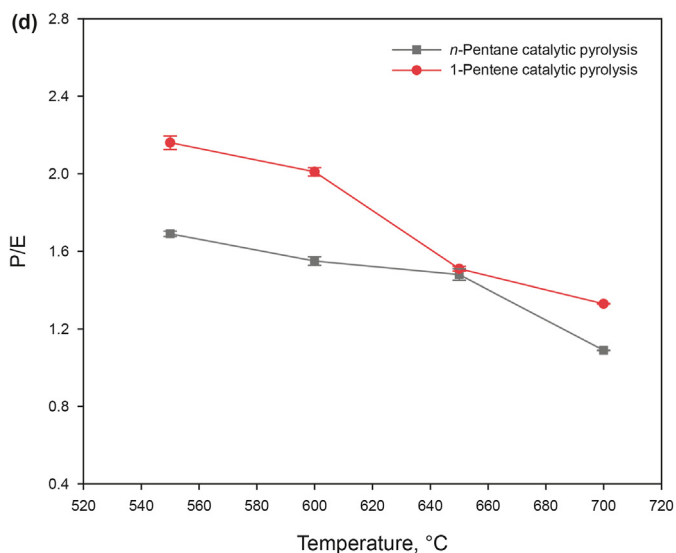
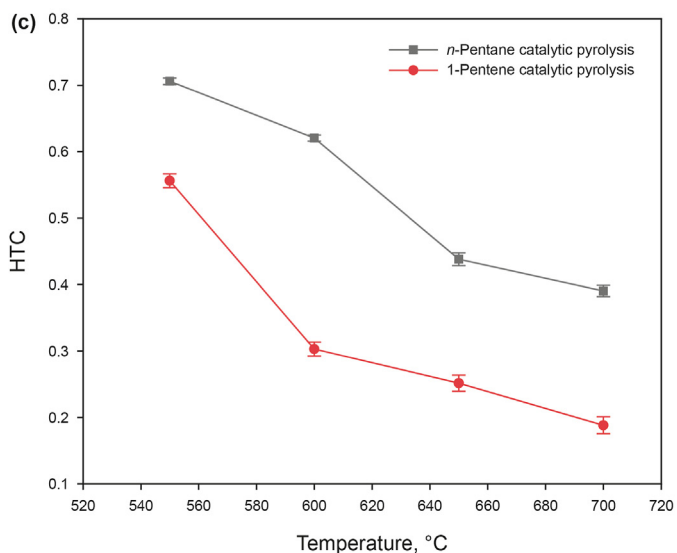
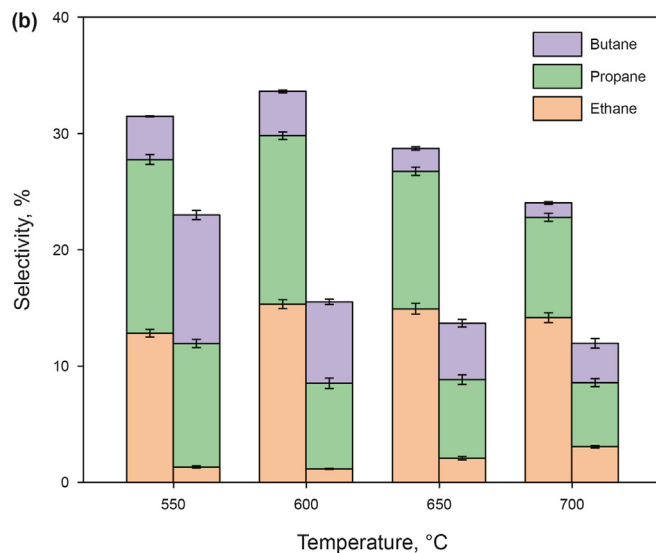
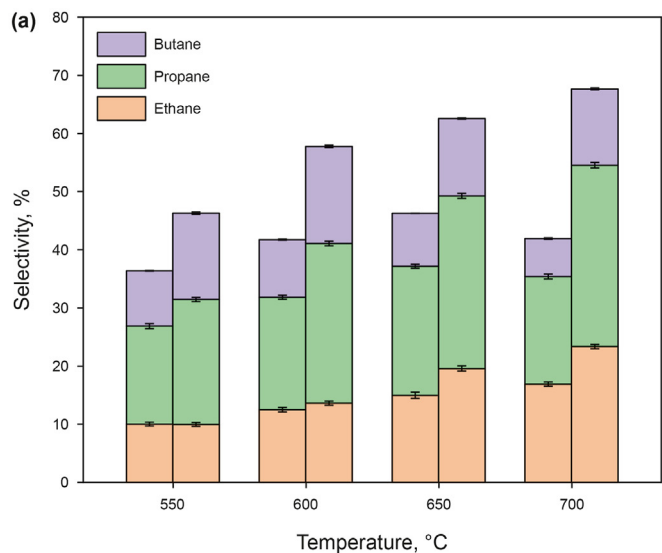


Fig. 5. (a) Selectivity of light olefins, (b) Selectivity of light alkanes, (c) HTC and (d) P/E at different reaction temperatures. In figures (a) and (b), the feedstock in the left bar graph is *n*-pentane and the feedstock in the right bar graph is 1-pentene.

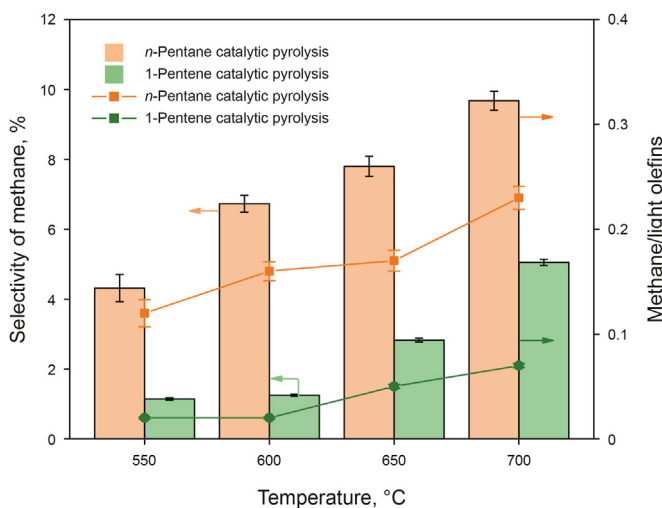


Fig. 6. Effect of reaction temperature on methane selectivity and mass ratio of methane to light olefins.

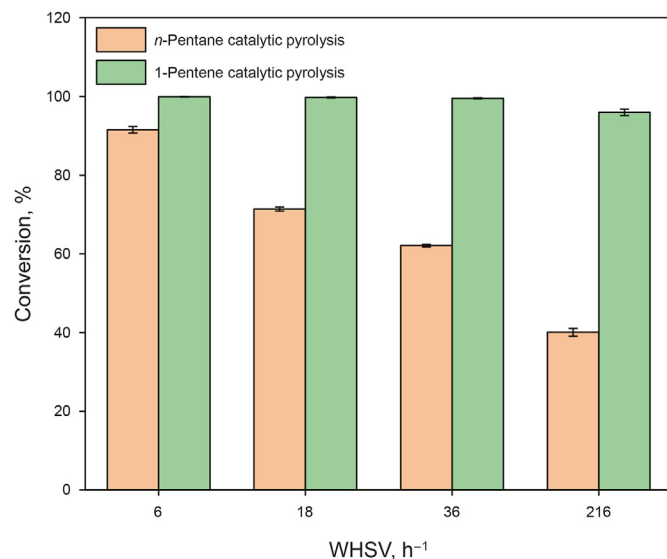


Fig. 7. Conversion of the catalytic pyrolysis of C₅ hydrocarbons at different WHSVs.

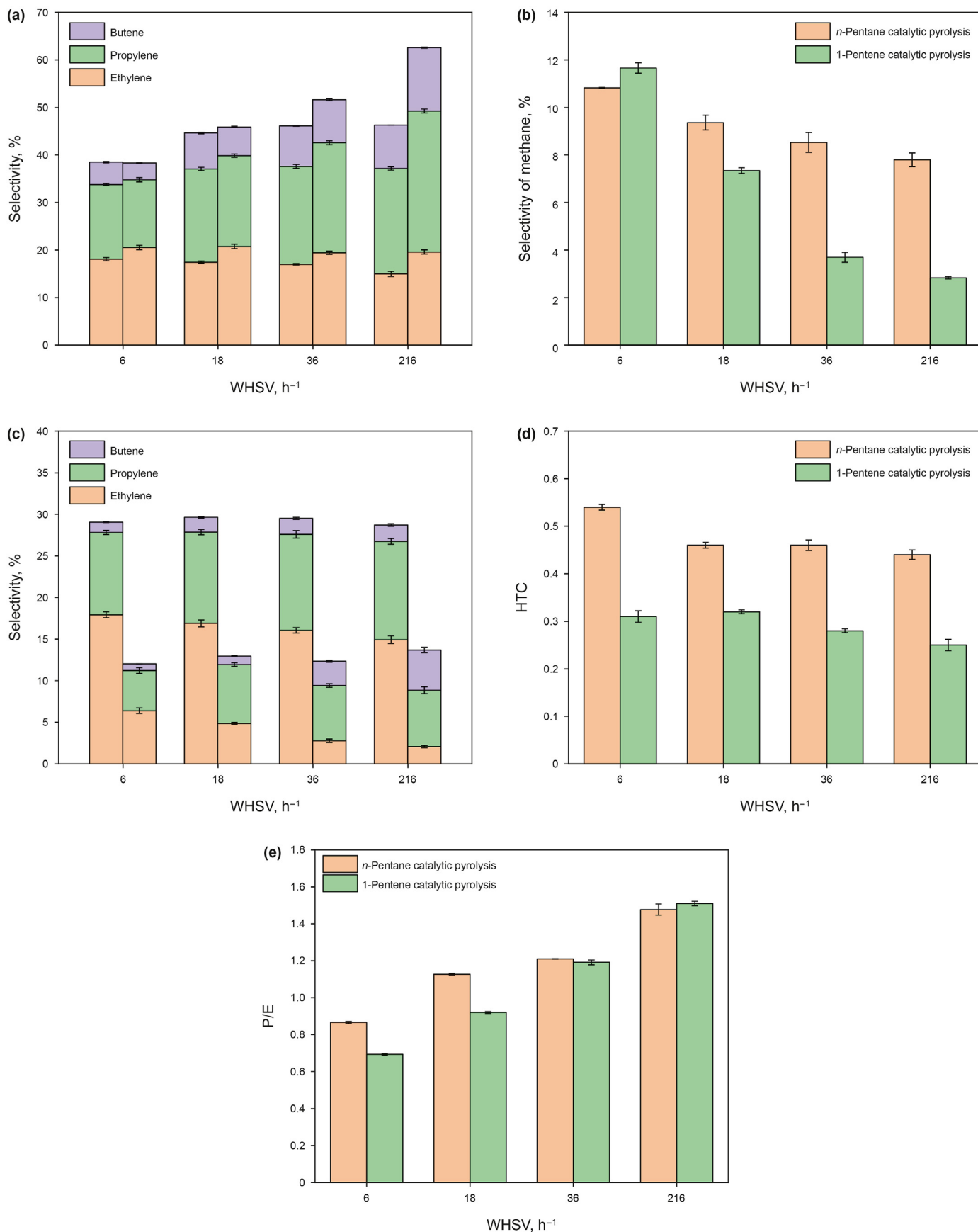
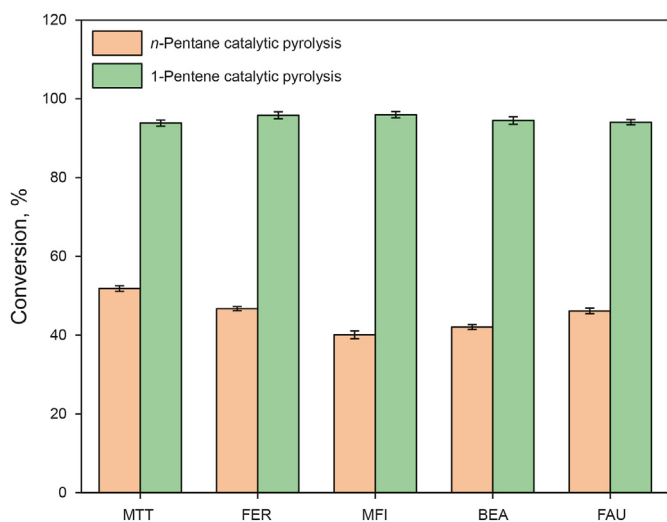


Fig. 8. (a) Selectivity of light olefins, (b) selectivity of methane, (c) selectivity of light alkanes, (d) HTC, and (e) P/E under different WHSVs. In figures (a) and (c), the feedstock in the left bar graph is *n*-pentane, and the feedstock in the right bar graph is 1-pentene.

Table 3
Selectivity of products from cracking of different hydrocarbons.

Feed	Reaction conditions	CH ₄	C ₂ H ₄	C ₃ H ₆	C ₄ H ₈	C ₂ –C ₄ olefins	Reference
1-hexene	Catalytic pyrolysis;	2.2	13.6	47.5	18.7	79.8	Le Van Mao et al. (2009)
1-tetradecene	630 °C;	1.3	19.1	44.8	17.1	81.0	
1-hexadecene	WHSV = 3.0 h ⁻¹	1.2	18.3	45.1	17.1	80.5	
1-octadecene		1.1	16.5	47.5	19.7	83.7	
<i>n</i> -butane	Catalytic pyrolysis;	13.6	32.1	21.0	5.1	58.1	Yoshimura et al. (2000)
<i>n</i> -pentane	650 °C;	8.0	35.4	19.0	5.7	60.0	
2-methyl-butane	W/F = 1.44–1.46 g s/mL	14.4	34.7	23.8	6.5	64.9	
<i>n</i> -pentane	Catalytic pyrolysis; 650 °C;	7.8	15.0	22.1	9.1	46.2	Liu et al. (2021a)
2-methyl-butane	WHSV = 220 h ⁻¹	13.8	19.6	28.1	14.5	62.2	
<i>n</i> -pentane	Thermal cracking;	11.9	43.1	23.9	6.2	73.2	Zámstný et al. (2010)
<i>n</i> -heptane	810 °C;	8.1	54.4	20.0	5.9	80.4	
2-methylhexane	residence time = 0.2–0.4 s	12.0	30.3	21.4	12.9	64.6	

**Fig. 9.** Conversion of the catalytic pyrolysis of C₅ hydrocarbons on different zeolites.

hydrogen transfer reaction and improve the selectivity of light olefins. In addition, Fig. 10c shows that the P/E for the catalytic pyrolysis of C₅ hydrocarbons was high on MTT and FER zeolites with small pore size, which was in agreement with the findings in the literature (Thivasasith et al., 2019).

Fig. 10d shows that there is little deviation of methane selectivity for the *n*-pentane catalytic pyrolysis over different zeolites and it was about 7%, indicating that when the conversion is similar, the type of zeolite had little effect on the formation of methane from *n*-pentane catalytic pyrolysis. However, the selectivity of methane for the catalytic pyrolysis of 1-pentene increased with the increase in the maximum spherical diameter contained in the zeolite. The methane selectivity was in the order of MTT (1.83%) < FER (1.90%) < MFI (2.83%) < BEA (4.81%) < FAU (10.20%). For carbenium ion, the relative stability is in the order of tertiary carbon (CR₃⁺) > secondary carbon (CR₂H⁺) > primary carbon (CRH₂⁺) (Xu, 2013). Therefore, the primary carbenium ion can easily generate tertiary carbenium ion through the isomerization reaction during the catalytic pyrolysis, as shown in Scheme 5 (Ye, 2016). The branching index (BI, $n [i-C_4H_{10}]/n [n-C_4H_{10}]$) for the catalytic pyrolysis of C₅ hydrocarbons is shown in Fig. 10d. The BI for the catalytic pyrolysis of 1-pentene increased significantly with the

increase in the maximum spherical diameter contained in the zeolite due to the larger diffusion space provided by the large pore size zeolite for iso-alkanes (as shown in Table 4). Meanwhile, Table 3 shows that isomeric hydrocarbons were easily demethylated, resulting in high methane selectivity (Cordero-Lanzac et al., 2018; Liu et al., 2021; Zámstný et al., 2010). Therefore, the selectivity of methane for the catalytic pyrolysis of 1-pentene on MTT and FER zeolites was lower than that on MFI, BEA and FAU zeolites, because the MTT and FER zeolites with small pore structure inhibit the isomerization reaction and reduce the methane produced by isomeric alkanes.

Based on investigating the effect of reaction conditions and zeolite types on the catalytic pyrolysis of C₅ hydrocarbons, the reaction pathways for the catalytic pyrolysis of C₅ hydrocarbons could be summarized, as shown in Scheme 6. C₅ hydrocarbons could generate methane, light alkanes and light olefins through cracking reactions (path I). Meanwhile, there are side reactions such as hydrogen transfer, isomerization, and secondary cracking in the catalytic pyrolysis of C₅ hydrocarbons. These side reactions will reduce light olefins and increase methane. However, increasing WHSV could reduce secondary cracking reaction (path II) and hydrogen transfer reaction (path III), and selecting MTT and FER zeolites with small pore size could inhibit hydrogen transfer reaction (path III) and isomerization reaction (path IV). Therefore, we suggested that zeolite with low hydrogen transfer activity and catalytic pyrolysis process with high WHSV will be conducive to maximize light olefins and to decrease methane.

4. Conclusion

The aim of this study is to find an optimal zeolite and reaction condition for the higher selectivity conversion of C₅ hydrocarbons to high value-added light olefins by catalytic pyrolysis. Firstly, the generation pathways of light olefins and methane from the catalytic pyrolysis of C₅ hydrocarbons were detailedly analyzed. It was found that methane is formed by breaking the C₁–C₂ bond at the end. For the catalytic pyrolysis of *n*-pentane and 1-pentene, the fracture ratios of the C₁–C₂ bond at the end were 23% and 22%, respectively. Therefore, the methane would be less tended to be formed by reducing the fracture ration of C₁–C₂ bond at the end.

After that, the effects of reaction conditions and zeolite types on the catalytic pyrolysis of C₅ hydrocarbons were investigated. It could be discovered that the break of the C₁–C₂ bond at the end could be promoted with increasing the reaction temperature,

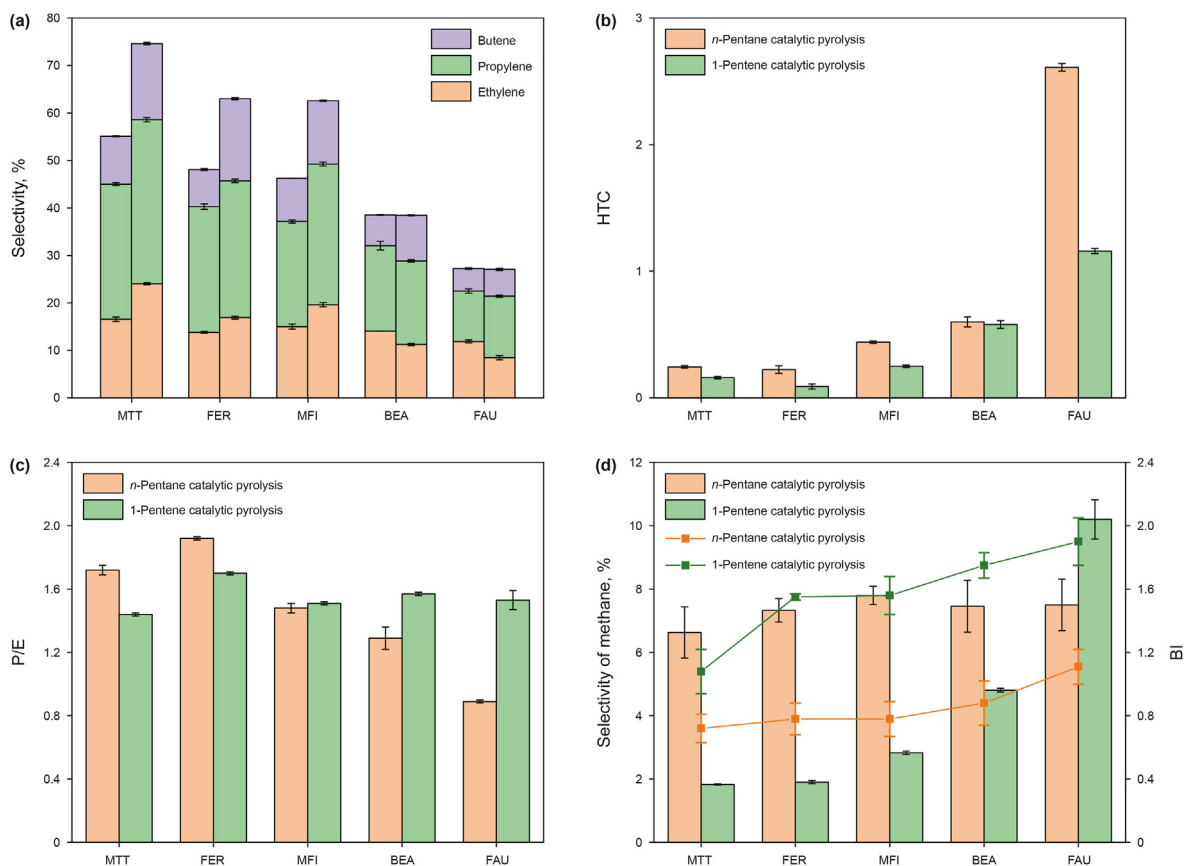
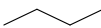
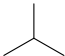
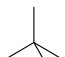
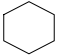


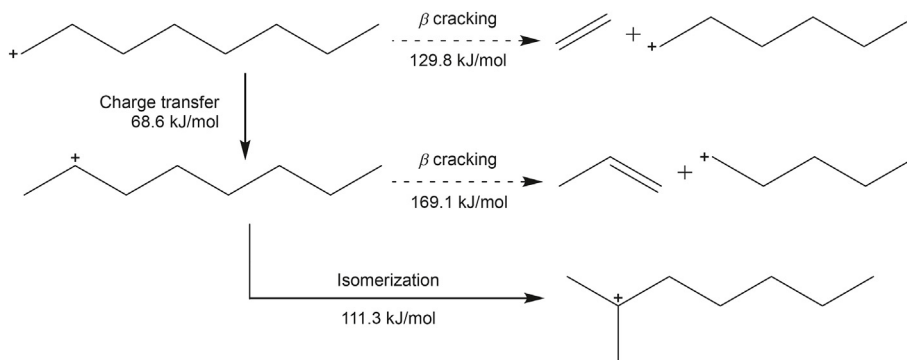
Fig. 10. (a) Selectivity of light olefins, (b) HTC, (c) P/E, and (d) selectivity of methane on different zeolites. In figure (a), the feedstock in the left bar graph is *n*-pentane, and the feedstock in the right bar graph is 1-pentene.

Table 4
Diffusion energy barriers (E_D) in MFI and FAU zeolite of alkane and cycloalkane (Yuan et al., 2011).

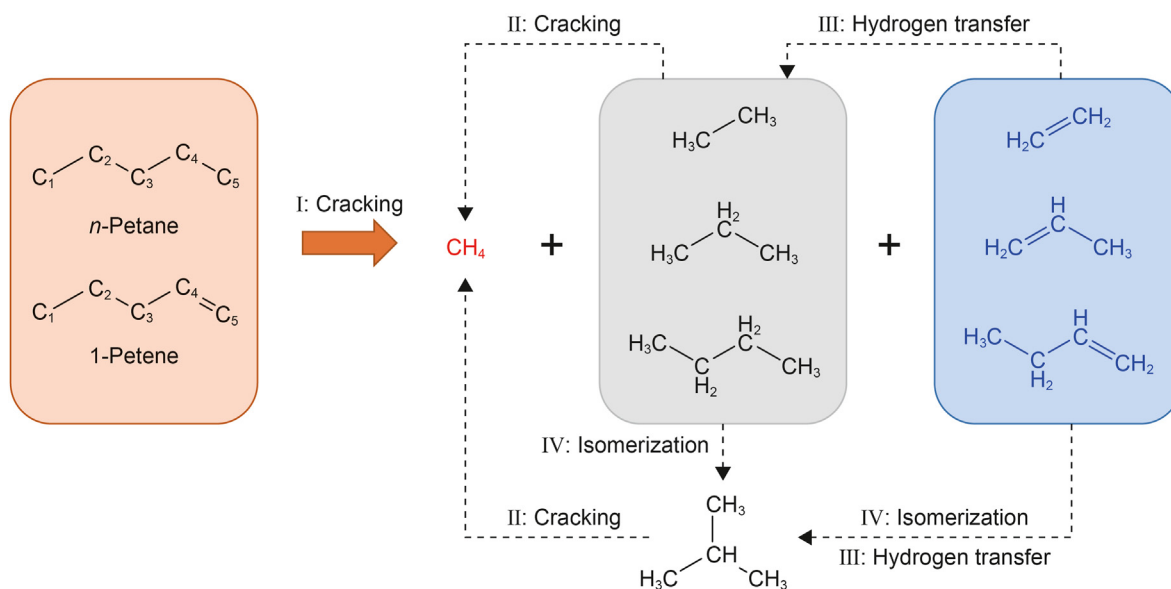
Molecule	$a \times b \times c / (\text{nm} \times \text{nm} \times \text{nm})$	$E_D, \text{kJ} \cdot \text{mol}^{-1}$	
		In MFI	In FAU
	$0.408 \times 0.45 \times 0.785$	11.051	7.619
	$0.505 \times 0.603 \times 0.663$	20.009	11.846
	$0.590 \times 0.605 \times 0.664$	87.278	8.707
	$0.495 \times 0.663 \times 0.733$	88.570	6.530

resulting the increase rate of methane was higher than that of light olefins. On the contrary, 90% of the hydrogen transfer reaction could be inhibited by increasing the WHSV and selecting MTT zeolite with 1D topology and FER zeolite with 2D topology. Correspondingly, the selectivity of light olefins for the catalytic pyrolysis of *n*-pentane and 1-pentene would be increased to 55.12% and 74.60%, respectively. Moreover, the fracture ratio of the C_1-C_2 bond at the end of hydrocarbon molecules was reduced, resulting in the selectivity of methane was reduced to 6.63% and 1.83%.

Therefore, it is preferred to select a zeolite with low hydrogen transfer activity, and improve the WHSV at an appropriate reaction temperature in order to maximize light olefins and to decrease methane during C_5 hydrocarbons catalytic pyrolysis process.



Scheme 5. Subsequent reaction of octyl carbenium ion (Ye, 2016).



Scheme 6. Reaction pathways for catalytic pyrolysis of C₅ hydrocarbons.

Acknowledgements

This work is supported by Program of China National Petroleum Corporation (2020B-2012; 2022ZS27) and the General Program of National Natural Science Foundation of China (22178385).

References

- Bortnovsky, O., Sazama, P., Wichterlova, B., 2005. Cracking of pentenes to C₂–C₄ light olefins over zeolites and zeotypes. *Appl. Catal. Gen.* 287 (2), 203–213. <https://doi.org/10.1016/j.apcata.2005.03.037>.
- Chu, Y.Y., Xue, N.H., Xu, B.L., et al., 2016. Mechanism of alkane H/D exchange over zeolite H-ZSM-5 at low temperature: a combined computational and experimental study. *Catal. Sci. Technol.* 6 (14), 5350–5363. <https://doi.org/10.1039/c6cy00467a>.
- Cordero-Lanzac, T., Aguayo, A.T., Gayubo, A.G., et al., 2018. Simultaneous modeling of the kinetics for *n*-pentane cracking and the deactivation of a HZSM-5 based catalyst. *Chem. Eng. J.* 331, 818–830. <https://doi.org/10.1016/j.cej.2017.08.106>.
- Corma, A., Melo, F.V., Sauvanoud, L., et al., 2004. Different process schemes for converting light straight run and fluid catalytic cracking naphthas in a FCC unit for maximum propylene production. *Appl. Catal. Gen.* 265 (2), 195–206. <https://doi.org/10.1016/j.apcata.2004.01.020>.
- Corma, A., Monton, J.B., Orchilles, A.V., 1985. Cracking of *n*-heptane on a hzsm-5 zeolite. The influence of acidity and pore structure. *Appl. Catal.* 16 (1), 59–74. [https://doi.org/10.1016/s0166-9834\(00\)84070-1](https://doi.org/10.1016/s0166-9834(00)84070-1).
- Corma, A., González-Alfaro, V., Orchillés, A.V., 1999. The role of pore topology on the behaviour of FCC zeolite additives. *Appl. Catal. Gen.* 187 (2), 245–254. [https://doi.org/10.1016/S0926-860X\(99\)00226-4](https://doi.org/10.1016/S0926-860X(99)00226-4).
- Corma, A., Mengual, J., Miguel, P.J., 2013. IM-5 zeolite for steam catalytic cracking of naphtha to produce propene and ethene. An alternative to ZSM-5 zeolite. *Appl. Catal. Gen.* 460–461, 106–115. <https://doi.org/10.1016/j.apcata.2013.02.030>.
- Corma, A., Corresa, E., Mathieu, Y., et al., 2017. Crude oil to chemicals: light olefins from crude oil. *Catal. Sci. Technol.* 7 (1), 12–46. <https://doi.org/10.1039/c6cy01886f>.
- Feng, B., Wei, Y.C., Song, W.Y., et al., 2022. A review on the structure-performance relationship of the catalysts during propane dehydrogenation reaction. *Petrol. Sci.* 19 (2), 819–838. <https://doi.org/10.1016/j.petsci.2021.09.015>.
- Haag, W.O., Dessau, R.M., Lago, R.M., 1991. Kinetics and mechanism of paraffin cracking with zeolite catalysts. *Stud. Surf. Sci. Catal.* 60, 255–265. [https://doi.org/10.1016/s0167-2991\(08\)61903-5](https://doi.org/10.1016/s0167-2991(08)61903-5).
- Hou, X., Qiu, Y., Zhang, X.W., et al., 2017. Analysis of reaction pathways for *n*-pentane cracking over zeolites to produce light olefins. *Chem. Eng. J.* 307, 372–381. <https://doi.org/10.1016/j.cej.2016.08.047>.
- Hou, X., Ni, N., Wang, Y., et al., 2019. Roles of the free radical and carbenium ion mechanisms in pentane cracking to produce light olefins. *J. Anal. Appl. Pyrol.* 138, 270–280. <https://doi.org/10.1016/j.jaap.2019.01.009>.
- Huang, X., Aihemaitijiang, D., Xiao, W.D., 2015. Reaction pathway and kinetics of C₃–C₇ olefin transformation over high-silicon HZSM-5 zeolite at 400–490 °C. *Chem. Eng. J.* 280, 222–232. <https://doi.org/10.1016/j.cej.2015.05.124>.
- Jung, J.S., Kim, T.J., Seo, G., 2004. Catalytic cracking of *n*-octane over zeolites with different pore structures and acidities. *Kor. J. Chem. Eng.* 21 (4), 777–781. <https://doi.org/10.1007/BF02705520>.
- Koyama, T.R., Hayashi, Y., Horie, H., et al., 2010. Key role of the pore volume of zeolite for selective production of propylene from olefins. *Phys. Chem. Chem. Phys.* 12 (11), 2541–2554. <https://doi.org/10.1039/b921927g>.
- Krannila, H., Haag, W.O., Gates, B.C., 1992. Monomolecular and bimolecular mechanisms of paraffin cracking: *n*-butane cracking catalyzed by HZSM-5. *J. Catal.* 135 (1), 115–124. [https://doi.org/10.1016/0021-9517\(92\)90273-k](https://doi.org/10.1016/0021-9517(92)90273-k).
- Kubo, K., Iida, H., Namba, S., Igarashi, A., 2012. Selective formation of light olefin by *n*-heptane cracking over HZSM-5 at high temperatures. *Microporous Mesoporous Mater.* 149 (1), 126–133. <https://doi.org/10.1016/j.micromeso.2011.08.021>.
- Le Van Mao, R., Muntasar, A., Yan, H.T., et al., 2009. Catalytic cracking of heavy olefins into propylene, ethylene and other light olefins. *Catal. Lett.* 130 (1–2), 86–92. <https://doi.org/10.1007/s10562-009-9911-4>.
- Li, C.Y., Yang, C.H., Shan, H.H., 2007. Maximizing propylene yield by two-stage riser catalytic cracking of heavy oil. *Ind. Eng. Chem. Res.* 46 (14), 4914–4920. <https://doi.org/10.1021/ie061420l>.
- Lin, L.F., Qiu, C.F., Zhuo, Z.X., et al., 2014. Acid strength controlled reaction pathways for the catalytic cracking of 1-butene to propene over ZSM-5. *J. Catal.* 309, 136–145. <https://doi.org/10.1016/j.jcat.2013.09.011>.
- Lin, L.F., Zhao, S.F., Zhang, D.W., et al., 2015. Acid strength controlled reaction pathways for the catalytic cracking of 1-pentene to propene over ZSM-5. *ACS Catal.* 5 (7), 4048–4059. <https://doi.org/10.1021/cs501967r>.
- Liu, M.J., Wang, G., Zhang, Z.D., et al., 2021a. Analysis of reaction performance of high efficient pyrolysis of C₅ alkanes to light olefins. *J. Chem. Ind. Eng.* 72 (10), 5172–5182. <https://doi.org/10.11949/0438-1157.20210488> (in Chinese).
- Liu, M.J., Wang, G., Zhang, Z.D., et al., 2021b. Study on hydrogen transfer reaction in C₅ hydrocarbons catalytic pyrolysis. *J. Fuel Chem. Technol.* 49 (1), 104–112. <https://doi.org/10.19906/j.cnki.jfct.2021006> (in Chinese).
- Luo, Y.R., 2005. Chemical bond energy data handbook. *Scientia* 50, 759. <https://doi.org/10.3321/j.issn:0023-074X.2005.08.021> (in Chinese).
- Miyaji, A., Iwase, Y., Nishitoba, T., et al., 2015. Influence of zeolite pore structure on product selectivities for protolysis and hydride transfer reactions in the cracking of *n*-pentane. *Phys. Chem. Chem. Phys.* 17 (7), 5014–5032. <https://doi.org/10.1039/c4cp04438j>.
- Potapenko, O.V., Doronin, V.P., Sorokina, T.P., et al., 2016. A study of intermolecular hydrogen transfer from naphthenes to 1-hexene over zeolite catalysts. *Appl. Catal. Gen.* 516, 153–159. <https://doi.org/10.1016/j.apcata.2016.02.028>.
- Primo, A., Garcia, H., 2014. Zeolites as catalysts in oil refining. *Chem. Soc. Rev.* 43 (22), 7548–7561. <https://doi.org/10.1039/c3cs60394f>.
- Rownaghi, A.A., Rezaei, F., Hedlund, J., 2012. Selective formation of light olefin by *n*-hexane cracking over HZSM-5: influence of crystal size and acid sites of nano- and micrometer-sized crystals. *Chem. Eng. J.* 191, 528–533. <https://doi.org/10.1016/j.cej.2012.03.023>.
- Sadrameli, S.M., 2016. Thermal/catalytic cracking of liquid hydrocarbons for the production of olefins: a state-of-the-art review II: catalytic cracking review. *Fuel* 173, 285–297. <https://doi.org/10.1016/j.fuel.2016.01.047>.
- Sundberg, J., Standl, S., von Aretin, T., et al., 2018. Optimal process for catalytic cracking of higher olefins on ZSM-5. *Chem. Eng. J.* 348, 84–94. <https://doi.org/10.1016/j.cej.2018.04.060>.
- Thivasasith, A., Maihom, T., Pengpanich, S., et al., 2019. Nanocavity effects of various

- zeolite frameworks on *n*-pentane cracking to light olefins: combination studies of DFT calculations and experiments. *Phys. Chem. Chem. Phys.* 21 (40), 22215–22223. <https://doi.org/10.1039/c9cp03871j>.
- Wang, G., Xu, C.M., Gao, J.S., 2008. Study of cracking FCC naphtha in a secondary riser of the FCC unit for maximum propylene production. *Fuel Process. Technol.* 89 (9), 864–873. <https://doi.org/10.1016/j.fuproc.2008.02.007>.
- Wei, X.L., Zhang, J.L., Mao, A.G., et al., 2014. Investigation on influence factors of methane formation in naphtha catalytic cracking. *Pet. Process. Petrochem.* 45 (3), 1–5. <https://doi.org/10.3969/j.issn.1005-2399.2014.03.001> (in Chinese).
- Xu, Y.H., 2013. *Chemistry & Process of Catalytic Cracking*. Science Press, Beijing (in Chinese).
- Yoshimura, Y., Kijima, N., Hayakawa, T., et al., 2000. Catalytic cracking of naphtha to light olefins. *Catal. Surv. Jpn.* 4 (2), 157–167. <https://doi.org/10.1023/A:1011463606189>.
- Ye, W.Z., 2016. *The Primary Exploration on the Chemical Structure and Refining Properties of Different Types of Petroleum Molecules*. Research Institute of Petroleum Processing, Beijing (in Chinese).
- Yuan, S., Long, J., Tian, H.P., et al., 2011. Molecular dimensions of hydrocarbons and a primary study on its relationship to diffusion energy barriers in zeolites. *Acta Petrol. Sin.: Pet. Process. Sect.* 27 (3), 376–380. <https://doi.org/10.3969/j.issn.1001-8719.2011.03.008> (in Chinese).
- Zámostný, P., Bělohav, Z., Starkbaumová, L., et al., 2010. Experimental study of hydrocarbon structure effects on the composition of its pyrolysis products. *J. Anal. Appl. Pyrol.* 87 (2), 207–216. <https://doi.org/10.1016/j.jaap.2009.12.006>.
- Zhang, J., Chen, T., Jiao, Y., et al., 2021. Improved activity of Ni-Mo/SiO₂ bimetallic catalyst synthesized via sol-gel method for methylcyclohexane cracking. *Petrol. Sci.* 18 (5), 1530–1542. <https://doi.org/10.1016/j.petsci.2021.08.009>.
- Zhang, R., Wang, Z.X., Liu, H.Y., et al., 2016. Thermodynamic equilibrium distribution of light olefins in catalytic pyrolysis. *Appl. Catal. Gen.* 522, 165–171. <https://doi.org/10.1016/j.apcata.2016.05.009>.
- Zhu, X., Liu, S., Song, Y., et al., 2005. Catalytic cracking of C₄ alkenes to propene and ethene: influences of zeolites pore structures and Si/Al₂ ratios. *Appl. Catal. Gen.* 288 (1–2), 134–142. <https://doi.org/10.1016/j.apcata.2005.04.050>.